Arabian Journal of Chemistry (2014) xxx, xxx–xxx

King Saud University

Arabian Journal of Chemistry

www.ksu.edu.sa
www.sciencedirect.com

ORIGINAL ARTICLE

Kinetics and equilibrium study for the adsorption of textile dyes on coconut shell activated carbon

Aseel M. Aljeboree [a], Abbas N. Alshirifi [b], Ayad F. Alkaim [a,*]

[a] *Department of Chemistry, College of Sciences for Women, Babylon University, Hilla, Iraq*
[b] *Department of Chemistry, College of Sciences, Babylon University, Hilla, Iraq*

Received 29 June 2013; accepted 28 January 2014

KEYWORDS

Activated carbon;
Adsorption;
Isotherm;
Kinetics;
Thermodynamics

Abstract The preparation of activated carbon from coconut husk with H_2SO_4 activation (CSAC) and its ability to remove textile dyes (maxilon blue GRL, and direct yellow DY 12), from aqueous solutions were reported in this study. The adsorbent was characterized with Fourier transform infrared spectrophotometer (FT-IR), and scanning electron microscope (SEM). Various physiochemical parameters such as, contact time, initial dye concentration, adsorbent dosage, particle size, pH of dye solution and temperature were investigated in a batch-adsorption technique. Result showed that the adsorption of both GRL and DY 12 dyes was favorable at acidic pH. The adsorption uptake was found to increase with increase in initial dye concentration, and contact time but decreases with the amount of adsorbent, particle size, and temperature of the system. The chemisorption, intra-particle diffuse, pseudo-first-order and pseudo-second-order kinetic models were applied to test the experimental data. The pseudo-second order exhibited the best fit for the kinetic studies, which indicates that adsorption of (GRL, and DY 12) is limited by chemisorption process. The equilibrium data were evaluated using Langmuir, Freundlich, Temkin and Fritz–Schlunder isotherms. The Fritz–Schlunder model best describes the uptake of (GRL and DY 12) dye, which implies that the adsorption of textiles dyes in this study onto coconut husk activated carbon is heterogeneous with multi-layers. Thermodynamic parameters such as Gibbs free energy, enthalpy and entropy were determined. It was found that (GRL and DY 12) dye adsorption was spontaneous and endothermic.

1. Introduction

Water pollution is one of the most undesirable environmental problems in the world and it requires solutions. Textile industries produce a lot of wastewater, which contains a number of contaminants, including acidic or caustic dissolved solids, toxic compounds, and any different dyes, many of these dyes are carcinogenic, mutagenic, and teratogenic and also toxic to human beings, fish species, and microorganisms. Hence, their

* Corresponding author. Tel./fax: +964 7801324986.
E-mail address: alkaim@iftc.uni-hannover.de (A.F. Alkaim).

Peer review under responsibility of King Saud University.

ELSEVIER Production and hosting by Elsevier

1878-5352 © 2014 Production and hosting by Elsevier B.V. on behalf of King Saud University.
http://dx.doi.org/10.1016/j.arabjc.2014.01.020

Please cite this article in press as: Aljeboree, A.M. et al., Kinetics and equilibrium study for the adsorption of textile dyes on coconut shell activated carbon. Arabian Journal of Chemistry (2014), http://dx.doi.org/10.1016/j.arabjc.2014.01.020

removal from aquatic wastewater becomes environmentally important (Konicki et al., 2013).

Large quantities of dangerous dyes, pigments and metals originated from dye manufacturing, textile as well as pulp and paper industries are emitted into wastewaters. This makes treating water contamination difficult , because the color tends to persist even after the conventional removal processes (Visa et al., 2010). The dye contaminations in water tend to prevent light penetration and therefore, affect photosynthesis considerably (Banerjee and Chattopadhyaya, 2013; Hajati et al., 2014; Hameed et al., 2013). Due to the wide application of dye compound and their numerous hazard and toxic derivatives, the cleaning of wastewater from color dyestuff becomes environmentally important (Ghaedi et al., 2013). Although, synthetic origins aromatic dyes are even biologically non-degradable and their treatment by other effective conventional procedure is impossible.

There are several methods available for color removal from waters and wastewaters such as membrane separation, aerobic and anaerobic degradation using various microorganisms, chemical oxidation, coagulation and flocculation, and reverse osmosis. Some of these techniques have been shown to be effective however they have some limitations such as excess amount of chemical usage, accumulation of concentrated sludge that has serious disposal problems and lack of effective color reduction. The adsorption technique, which is based on the transfer of pollutants from the solution to the solid phase, is known as one of the efficient and general wastewater treatment method (Ghaedi et al., 2012). The method is superior to other dye removal techniques in terms of initial cost, simplicity of design, ease of operation, and non-toxicity of the utilized adsorbents compared to other conventional wastewater treatment methods (Kismir and Aroguz, 2011). The cost effectiveness, availability and adsorptive properties are the main criteria in selection of an adsorbent to remove organic compounds from wastewaters (Demirbas et al., 2008; Ghaedi et al., 2012), also application of adsorption procedure especially based on non-toxic and green adsorbent with high surface area and reactive surface atom is a great demand (Chiou and Chuang, 2006).

Activated carbon, a widely used adsorbent in industrial processes, is composed of a microporous, homogenous structure with high surface area and shows radiation stability (Iqbal and Ashiq, 2007). The process for producing high-efficiency activated carbon is not completely investigated in developing countries. Furthermore, there are many problems with the regeneration of used activated carbon. Nowadays, there is a great interest in finding inexpensive and effective alternatives to the existing commercial activated carbon (AlOthman et al., 2013). Exploring effective and low-cost activated carbon may contribute to environmental sustainability and offer benefits for future commercial applications. The costs of activated carbon prepared from biomaterials are very low compared to the cost of commercial activated carbon. Waste materials that have been successfully used to manufacture activated carbon in the recent past include waste wood (Acharya et al., 2009), bagasse (Tsai et al., 2001), coir pith (Namasivayam and Kavitha, 2002), orange peel (Khaled et al., 2009), coffee husk (Ahmad and Rahman, 2011), pine cone (Gecgel and Kolancilar, 2012), coconut tree (Senthilkumaar et al., 2006), sunflower seed hull (Thinakaran et al., 2008), pine-fruit shell (Royer et al., 2009), hazelnut husks, rice hulls, oil palm shell (Tan et al., 2008), and Coconut husk (Foo and Hameed, 2012).

The objective of this work is to study the static capacity of adsorption of textile dyes (GRL, and DY 12) by the prepared activated carbons derived by coconut shells (CSAC). The effects of contact time, initial dye concentration, mass dosage, temperature, and pH on the static adsorption of the dye onto the prepared CSAC were examined. The pseudo-first order and pseudo-second order models are used to correlate the adsorption kinetics data of GRL and DY 12 onto prepared activated carbons. The kinetics as well as the diffusion parameters are also evaluated. Thermodynamic studies have also been performed to understand the processes of removal of the selected dyes on CSAC.

2. Experimental

2.1. Materials and methods

Maxilon blue GRL [λ_{max} = 599 nm] and direct yellow DY 12 [λ_{max} = 403 nm] were obtained from Al-Hilla¸ Textile Company (Babylon, Iraq). The chemical structures of maxilon blue GRL and direct yellow DY 12 are shown in Fig. 1. Concentrations of dyes were determined by finding out the absorbance at the characteristic wavelength using a double beam UV/Vis spectrophotometer (UV–Visible spectrophotometer, Shimadzu 1650). Calibration curves were plotted between absorbance and concentration of the dye solution.

2.2. Preparation of H_2SO_4-activated carbon (CSAC)

Coconut shells are obtained from the Iraqis local markets and were used as precursors. Firstly, they were washed with distilled water to remove any adhering impurities, and then dried at 110 °C for 24 h followed by grinding and sieving in order to use particles size ranged between 1 mm and 2 mm. H_2SO_4/activated carbon sample (CSAC) was prepared via two steps: carbonization of dried precursor at 500 °C for 2 h in the absence of air using a muffle furnance (600 × 40 mm) at a rate of 10 °C/min up to 500 °C. The carbonized sample was cooled and soaked with certain weight of H_2SO_4 (20 g of carbonized sample with 60 g of H_2SO_4 (50%)) in 100 ml distilled water for 24 h at room temperature, followed by drying at 110 °C and finally activated at 600 °C for 4 h. Prepared sample was washed several times with distilled water till neutral filtrate and then dried at 110 °C to constant weight and finally stored in a clean dry glass bottle.

2.3. Characterization of prepared H_2SO_4-activated carbon (CSAC)

Infrared spectra of the adsorbents were obtained using a Fourier transform infrared spectrometer (FTIR-2000, PerkinElmer). For the FT-IR study, finely ground adsorbent has been intimately mixed with KBr (Merck) in a ratio of 1:100 in order to prepare a translucent pellet. From these FT-IR spectra the presence of functional groups on the adsorbent were confirmed. The surface morphology of the activated carbon particles was analyzed using a scanning electron microscope (JEOL-JSM-6380 LA, Japan). The carbon particles were mounted on sample

Please cite this article in press as: Aljeboree, A.M. et al., Kinetics and equilibrium study for the adsorption of textile dyes on coconut shell activated carbon. Arabian Journal of Chemistry (2014), http://dx.doi.org/10.1016/j.arabjc.2014.01.020

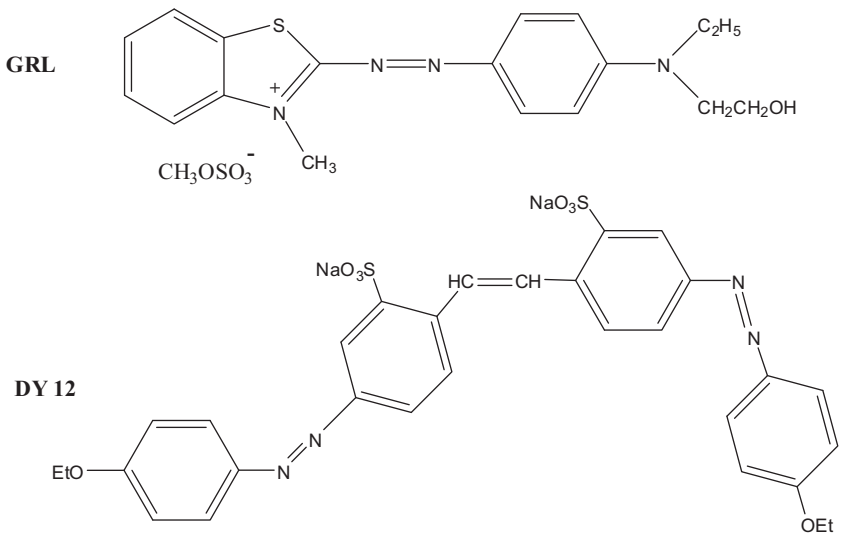

Figure 1 Chemical structures of both dyes maxilon blue (GRL), and direct yellow (DY 12).

stubs and coated with gold foil using a gold-coating machine (JEOL-JSM-420, Japan). The samples were then automatically analyzed using computer software.

2.4. Kinetic experiments

Adsorption kinetic experiments were carried out using shaker water bath. All of the dye solution was prepared with distilled water. Kinetic experiments were carried out by agitating 100 ml of solution of a constant dye concentration with 50 mg of CSAC at a constant agitation speed, 20 °C and natural pH. Agitation was made for 120 min, which is more than sufficient time to reach equilibrium at a constant stirring speed of 120 rpm. Preliminary experiments had shown that the effect of the separation time on the adsorbed amount of dye was negligible. Two milliliters of samples was drawn at suitable time intervals. The samples were then centrifuged for 15 min at 5000 rpm and the left out concentration in the supernatant solution was analysed using UV–vis spectrophotometer by monitoring the absorbance changes at a wavelength of maximum absorbance (599 and 403 nm for GRL and DY 12 respectively). Each experiment continued until equilibrium conditions were reached when no further decrease in the dye concentration was measured. Calibration curves were plotted between absorbance and concentration of the dye solution. It was investigated the effects of the following parameters to the removal rate of maxilon blue GRL and direct yellow DY 12 dyes on CSAC in the experiments.

2.5. Effect of different parameters of adsorption processes of GRL and DY 12 on CSAC

2.5.1. Effect of initial dye concentration

The initial tested concentrations of dyes were 2, 4, 6, 8, 10, 12, 14, and 16 mg/L for both dyes at different pH, temperature, particle size, and mass dosage.

2.5.2. Effect of pH

The effect of pH on the rate of color removal was analyzed in the pH range at 3, 6, 8 and 10 at 20 °C, 120 rpm, 50 mg of CSAC (particle size 75 μm) and 100 mL of dye concentration (2–16) mg/L. The pH was adjusted using 0.1 N NaOH and 0.1 N HCl solutions by using an Orion 920A pH-meter with a combined pH electrode. pH-meter was standardized with NBS buffers before every measurement.

2.5.3. Effect of solution temperature

The effect of temperature to the adsorption capacity of CSAC was carried out at 10, 20, 30, and 40 °C in a constant temperature bath at natural solution pH 6, 120 rpm 50 mg of CSAC (particle size 75 μm) and 100 mL of dye concentration (2–16) mg/L.

2.5.4. Effect of mass dosage

The effect of mass dosage was studied by agitating in different masses (0.005, 0.01, 0.05, and 0.5 g), at 20 °C, 120 rpm, 50 mg of CSAC (particle size 75 μm) and 100 mL of (DY 12 or GRL) dye concentration (2–16) mg/L.

2.5.5. Effect of particle size

The effect of particle size to the adsorption capacity of CSAC was carried out in (50, 75, and 106 μm), at 20 °C, pH 6, 120 rpm, 50 mg of CSAC and 100 mL of dye concentration (2–16) mg/L.

2.6. Data evaluation

Adsorption kinetics investigations were carried out by agitating 100 mL of GRL, and DY 12 dye solutions of known initial concentration with 0.5 g/L of adsorbent at a known temperature of 318 K, at pH of 6.0 ± 0.2 and at 120 rpm for different time intervals. The amount of dye adsorbed onto the adsorbent at equilibrium, q_e (mg/g), was calculated by the following expression:

$$q_e = \frac{(C_0 - C_e) * V}{w} \quad (1)$$

where C_0 and C_e are the initial and equilibrium dye concentrations in mg/L respectively, V is the volume of solution (L) and

W is the mass of the CSAC adsorbent (g), the amount of adsorption at time t, q_t (mg/g) was calculated by:

$$q_t = \frac{(C_0 - C_t) * V}{w} \quad (2)$$

where C_0 and C_t (mg/g) are the liquid phase concentrations of the dye at initial and any time t, respectively. V is the volume of solution (L) and W is the mass of the CSAC adsorbent (g).

3. Results and discussion

3.1. Surface characterizations

In order to detect the functionality present in CSAC prior to and after (GRL and DY 12) dyes adsorbed. Adsorption in the infrared (IR) region takes place (4000–400 cm^{-1}) due to the rotational and vibrational movement of the molecular groups and chemical bond of a molecule. The FT-IR spectra were obtained to evaluate qualitatively the chemical structures of CSAC. (Fig. 2(a)) shows the FT-IR spectrum of CSAC, which indicated various surface functional groups. The broadband at around 3500 cm^{-1} is typically attributed to hydroxyl groups. The region of the spectrum of 2220 cm^{-1} is attributed to alkyne group (C≡C). The region of the spectrum of 1612 cm^{-1} is attributed to axial deformation of carbonyl groups (C═O) (Cazetta et al., 2011). The presence of hydroxyl groups, carbonyl group, ethers and aromatic compounds is an evidence of the lignocellulosic structure of coconut shell as also observed in other materials such as Brazilian coconut shell (Cazetta et al., 2011), and jackfruit peel waste (Prahas et al., 2008), (Fig. 2(b and c) shows there is no real shift in our absorption peaks but the intensity becomes higher after absorption, this is indicated as a physical adsorption.

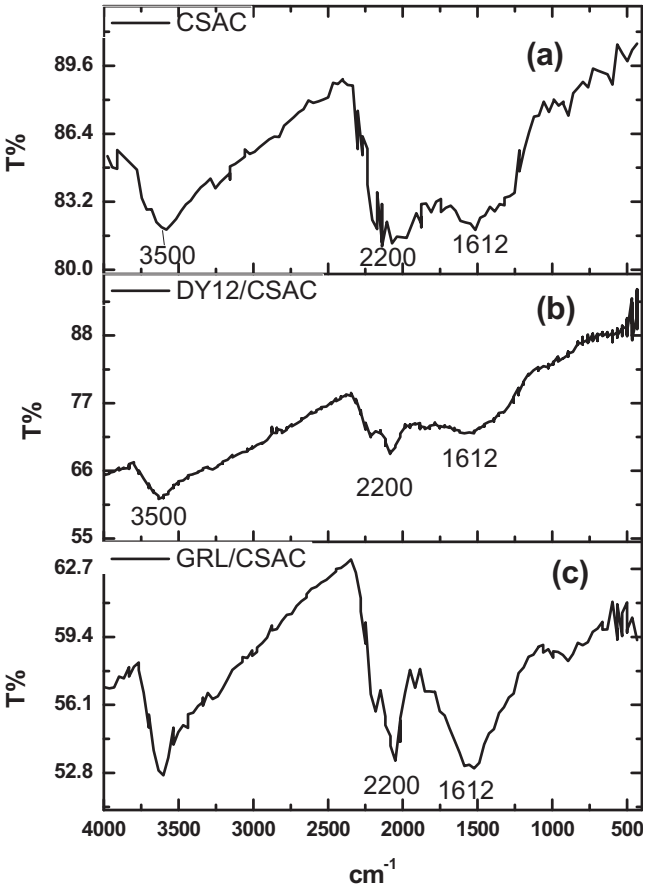

Figure 2 FT-IR spectra of (a) CSAC derived from coconut shell (b) DY 12 adsorbed on the surface of CSAC, and (c) GRL adsorbed on the surface of CSAC.

Scanning electron microscopy (SEM) has been a primary tool for characterizing the surface morphology and fundamental physical properties of the adsorbent. SEM of adsorbent material was taken before and after dye adsorption on CSAC (Fig. 3). From (Fig. 3a), it is clear, there is a good possibility for dyes to be trapped and adsorbed into these pores. The SEM pictures of adsorbed samples show very distinguished dark spots which can be taken as a sign for effective adsorption of dye molecules in the cavities and pores of this adsorbent. The micrographs presented in (Figs. 3b and c) show clearly the dye-loaded adsorbent coated by dye molecules over the whole surface at natural pH conditions. The dye molecules seem to have formed a void-free film masking the reliefs of particles and porosity of the aggregates (Kismir and Aroguz, 2011).

3.2. Adsorption kinetics modeling

Study of adsorption kinetics is important because the rate of adsorption (which is one of the criteria for efficiency of adsorbent) and also the mechanism of adsorption can be concluded from kinetic studies. Fig. 4 shows the variation of the amount of adsorbed (q_t) as a function of time. The rate of adsorption for both dyes is high at initial times of adsorption. For both dyes most of adsorption takes place within 10 min which indicate that the rate of dye adsorption by CSAC is high.

In order to analyze the adsorption kinetics of GRL and DY 12 by CSAC the pseudo-first order (Lagergren, 1898), pseudo-second order (Ho and McKay, 1999), Elovich equation (Low, 1960), and intra-particle diffusion (Weber and Morris, 1963), were tested. The result of fitting is listed in Table 1. A simple kinetic analysis of adsorption (pseudo-first-order equation) is in the form:

$$q_t = q_e[1 - exp(k_f t)] \quad (3)$$

where q_t is the amount of adsorbate adsorbed at time t (mg g^{-1}), q_e is the adsorption capacity in the equilibrium (mg g^{-1}), k_f is the pseudo-first-order rate constant (min^{-1}), and t is the contact time (min).

A pseudo-second-order equation based on adsorption equilibrium capacity may be expressed in the form:

$$q_t = \frac{k_s q_e^2 t}{1 + k_s q_e t} \quad (4)$$

where K_s is the the pseudo-first-order rate constant (g gm^{-1} - min^{-1}), the initial sorption rate (ho, expressed in mg g^{-1} min^{-1}) can be obtained when t approaches to zero, Eq. (5)

$$h_0 = k_s q_e^2 \quad (5)$$

The Elovich equation used for general application to chemisorption. The equation has been applied satisfactorily to some chemisorption processes and has been found to cover a wide range of slow adsorption rates. The same equation is often valid for systems in which the adsorbing surface is heterogeneous, and is formulated as:

Please cite this article in press as: Aljeboree, A.M. et al., Kinetics and equilibrium study for the adsorption of textile dyes on coconut shell activated carbon. Arabian Journal of Chemistry (2014), http://dx.doi.org/10.1016/j.arabjc.2014.01.020

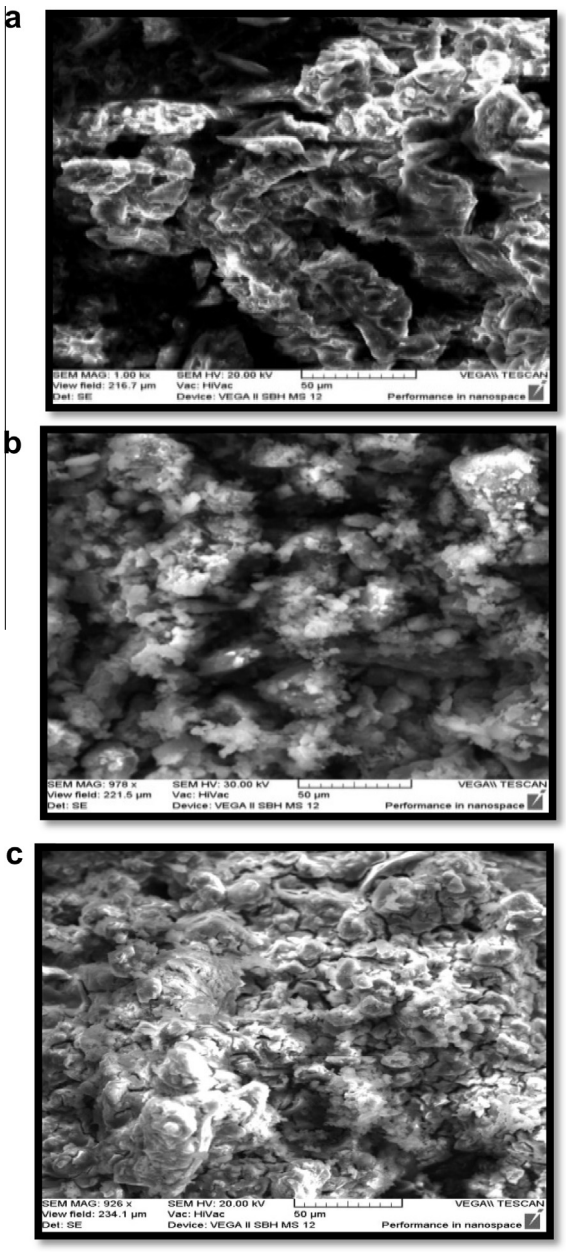

Figure 3 Scanning electron micrographs (SEM): (a) CSAC before adsorption process, (b) CSAC adsorbed with GRL and (c) CSAC adsorbed with DY 12.

$$q_t = \left(\frac{1}{\beta}\right) ln(\propto .\beta) + \left(\frac{1}{\beta}\right) ln(t) \tag{6}$$

The intra-particle diffusion model based on the theory proposed by Weber and Morris (Weber and Morris, 1963) was used to identify the diffusion mechanism. According to this theory, the adsorbate uptake q_t varies almost proportionally with the square root of the contact time, $t½$ rather than t, Eq.(7).

$$q_t = k_{id}\sqrt{t} + I \tag{7}$$

where I is the intercept and K_{id} (mg g^{-1} $min^{-1/2}$) is the intra-particle diffusion rate constant.

Fig. 4 represents the variation of dye adsorption on CSAC with shaking time (0–60 min) and initial dye solution concentration of 10.0 mg/L. Fig. 4 indicates that while the adsorption of dyes was quite rapid initially, the rate of adsorption became slower with the time and reached a constant value (equilibrium time). The initial faster rate may be due to the availability of the uncovered surface area of the adsorbents. (Kilic et al., 2011; Shi et al., 2013).

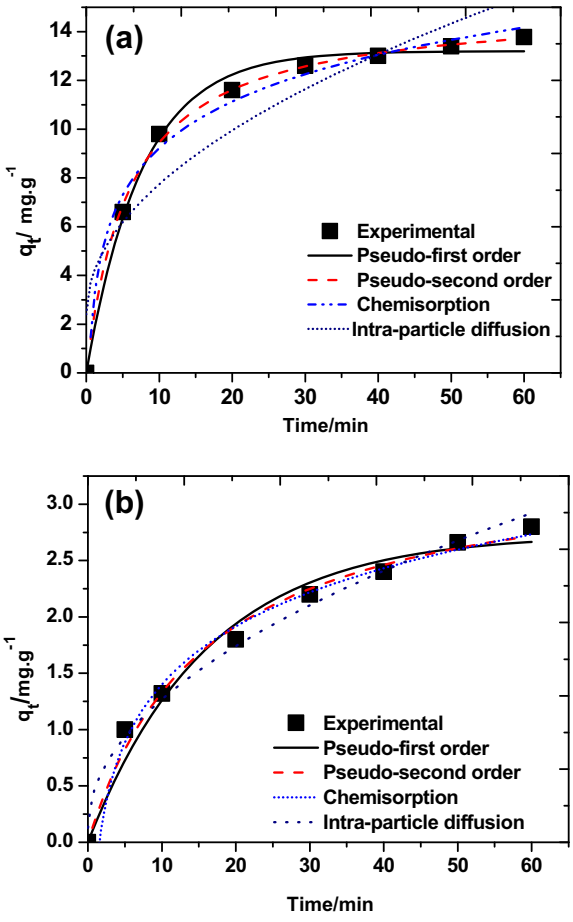

Figure 4 Adsorption rate curves (a) GRL dye, and (b) DY 12 dye: experimental conditions: pH 6, dye conc. 10 mg/L, particle size 75 μm, Temp. 293 K and mass catalyst 0.05 g).

All the experimental data showed better compliance with chemisorptions kinetic model for GRL and DY 12 in terms of higher correlation coefficient values $R^2 > 0.989$. Moreover, the q values calculated ($q_{e,cal}$) from pseudo first-order model were more consistent with the experimental q values ($q_{e,exp}$) than those calculated from the pseudo second-order model.

3.3. Effect of different parameters of adsorption processes of GRL and DY 12 on CSAC

3.3.1. Effect of pH

The effect pH was investigated on the adsorption of GRL and DY 12 on CSAC at a pH of 3–10 for 2 h. The result in Fig. 5 showed that maximum adsorption of GRL, and DY 12 was obtained at the lowest pH 3 while the lowest adsorption was at pH 10.

As the pH of the solution increases, adsorption of both dyes GRL and DY 12 was found to be decreasing; this was due to the extinction of the positive hydrogen ions thereby promoting

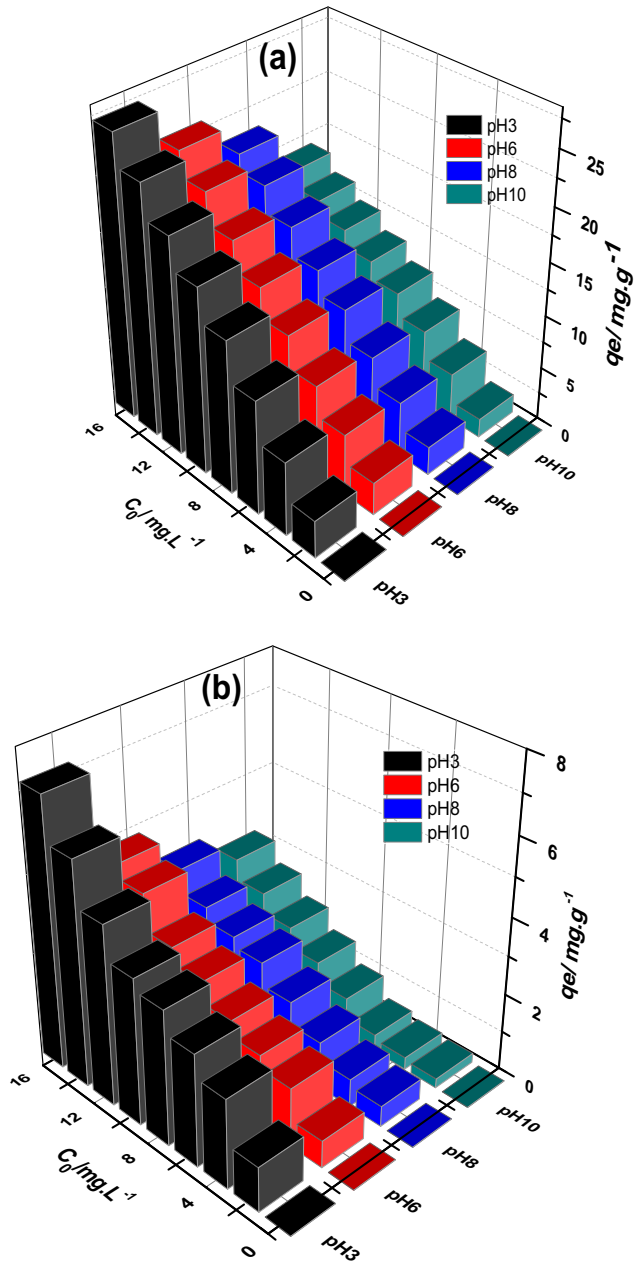

Figure 5 Effect of solution pH on adsorption (a) GRL, and (b) DY 12 experimental conditions: Temp. 293 K, CSAC dosage 50 mg/L, and particle size 75 μm.

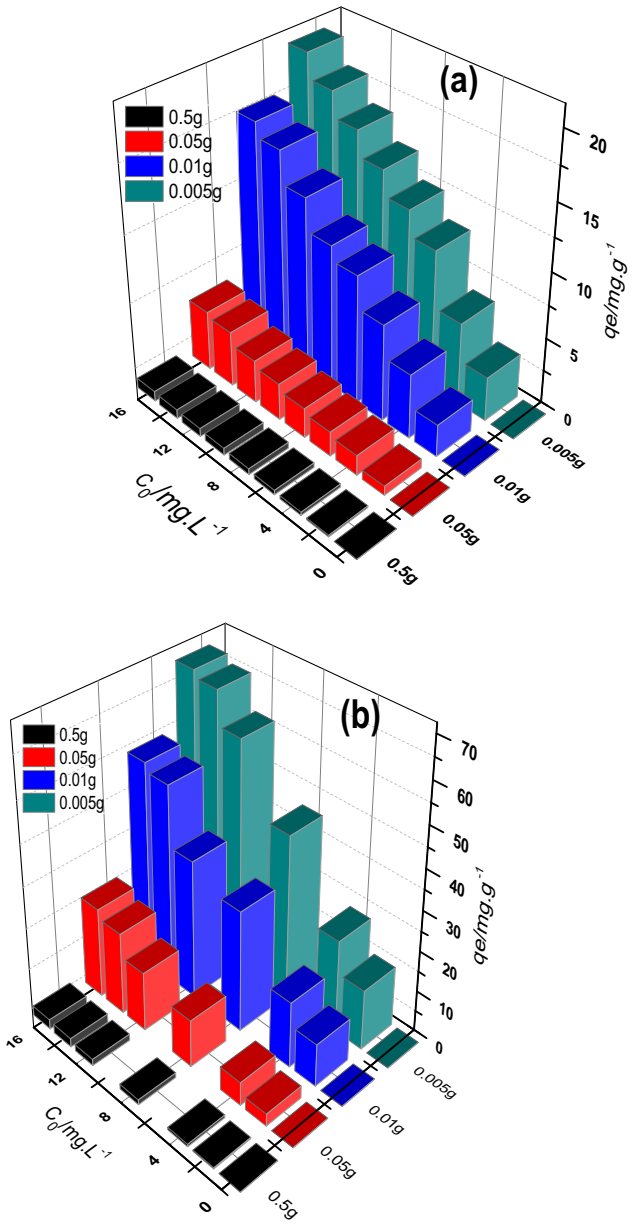

Figure 6 Effect of mass adsorbent on adsorption (a) GRL, and (b) DY 12 experimental conditions: Temp. 293 K, pH 6, and particle size 75 μm.

activities of electrostatic repulsion between the negative charges of both dye and the CSAC surface (Auta and Hameed, 2011). While at an acidic pH, the functional groups of activated carbon become protonated, which are mainly the carboxylic groups ($-COOH_2^+$), phenolic (($-OH_2^+$)) and chromenic group (Al-Degs et al., 2008). At pH 3, the surface charge of CSAC becomes more positively charged, which enhances (GRL and DY 12) adsorption through electrostatic attraction.

3.3.2. Effect of adsorbent dose

Fig. 6 shows the adsorption of both dyes GRL and DY 12 as a function of adsorbent dosage. It is apparent that by increasing the adsorbent dose the amount of adsorbed dye increases but adsorption density, the amount adsorbed per unit mass, decreases. It is readily understood that the number of available adsorption sites increases by increasing the adsorbent dose and it, therefore, results in an increase of the amount of adsorbed dye (Hameed et al., 2013). The decrease in adsorption density with an increase in the adsorbent dose is mainly because of adsorption sites remain unsaturated during the adsorption reaction whereas the number of sites available for adsorption site increases by increasing the adsorbent dose (Malik et al., 2007; Yener et al., 2006) .

3.3.3. Effect of particle size

Particle size of an adsorbent played a very important role in the adsorption capacity of dye. The relationship of adsorption capacity to particle size depends on two criteria: (i) the chemical

Table 1 Pseudo first-order, pseudo second-order, chemisorption and intraparticle diffusion model constants and correlation coefficients for (GRL and DY 12 dyes) adsorption onto CSAC.

Kinetic model	Dye	Parameters	Value	Standard error	R^2
Pseudo-first order	GRL	k_f (min^{-1})	0.13088	0.00934	0.99233
		q_e (mg g^{-1})	13.19959	0.21266	
	DY 12	k_f (min^{-1})	0.06179	0.00908	0.97437
		q_e (mg g^{-1})	2.73303	0.1311	
Pseudo-second order	GRL	ks (g mg^{-1} min^{-1})	0.01113	0.00066	0.99304
		q_e (mg g^{-1})	15.07327	0.19122	
		h_0 (mg g^{-1} min^{-1})	2.52877	-	
	DY 12	ks (g mg^{-1} min^{-1})	0.01837	0.00283	0.97400
		q_e (mg g^{-1})	3.43605	0.18306	
		h_0 (mg g^{-1} min^{-1})	0.21688	-	
Chemisorption	GRL	α (mg g^{-1} min^{-1})	7.74641	0.70563	0.98955
		β (g min^{-1})	0.3616	0.028329	
	DY 12	α (mg g^{-1} min^{-1})	0.48945	0.1231	0.99057
		β (g min^{-1})	1.34518	0.06879	
Intra-particle diffusion	GRL	k_{id} (mg g^{-1} $min^{-0.5}$)	1.68632	0.24566	0.86823
	DY 12	k_{id} (mg g^{-1} $min^{-0.5}$)	0.36053	0.01328	0.99058

structure of the dye molecule (its ionic charge) and its chemistry (its ability to formhydrolyzed species) and (ii) the intrinsic characteristic of the adsorbent (its crystallinity, porosity and rigidity of the polymericchains) (Iqbal et al., 2011). Fig. 7 shows the effect of particle size on textile dye adsorption.

Fig. 7 shows Minimum particle size showed greater adsorption than larger size. Small size of adsorbent increases the surface area for adsorption. The increase in adsorption capacity with decreasing particle size suggests that the dye preferentially adsorbed on the outer surface and did not fully penetrate the particle due to steric hindrance of large dye molecules (Gouamid et al., 2013; Li et al., 2011; Rehman et al., 2013).

3.3.4. Effect of temperature

The effect of temperature on the adsorption of both dyes (GRL and DY 12) by CSAC was studied within the temperatures (10, 20, 30 and 40 °C) on adsorption at (2–16 mg/L) initial dye concentration, pH 6, results are shown in Fig. 8.

It was observed that the adsorption capacity of GRL on CSAC (Fig. 8a) was higher than that of DY 12 (Fig. 8b). This results may be ascribed to the vacant sites on AC used for adsorption were constant, and the molecular weight of GRL was higher than that of DY 12. Meanwhile, with the initial temperatures of dye solution increased from 10 to 40 °C, the adsorption capacities of GRL and DY 12 decreased this may causes an increase in the solubility of the dyes, resulted in a stronger interaction forces between dyes and solvent than those between dyes and CSAC (Dotto et al., 2012; Zhou et al., 2011; Zhou et al., 2014). A decrease in the adsorption of both dyes GRL and DY 12 with increasing temperature is related to the increasing Brownian movement of molecules in solution (Li et al., 2013). High temperature might also lead to the breaking of existing intermolecular hydrogen bonding between GRL and DY 12 and CSAC, which is an important contribution to the adsorption process (Li et al., 2013).

3.4. Thermodynamic study

The thermodynamic behaviors for adsorption of GRL and DY 12 on CSAC were further investigated. The thermodynamic parameters such as Gibbs free energy change ($\Delta G°$), enthalpy ($\Delta H°$), and entropy ($\Delta S°$) were calculated using the following equations:

$$\Delta G^0 = -RTlnK_0 \tag{8}$$

where k_0 is the apparent equilibrium constant, R is the gas constant (8.314 J/(molK)), and T is absolute temperatures (K). The apparent enthalpy ($\Delta H°$) of adsorption and entropy ($\Delta S°$) of adsorption were calculated from adsorption data at different temperatures using the Van't Hoff Eq. (9) as follows:

$$lnK_0 = \frac{-\Delta H^\circ}{RT} + \frac{\Delta S^\circ}{R} \tag{9}$$

The values of ln K_0 for thermodynamic calculations were obtained from equilibrium constant (K_s) for the adsorption as follows (Li et al., 2010):

$$K_s = \frac{q_e}{C_e} \times \frac{v_1}{v_2} \tag{10}$$

where v_1 is the activity coefficient of the adsorbed solute, and v_2 is the activity coefficient of the solute in equilibrium suspension. The ratio of activity coefficients was assumed to be uniform in the dilute range of the solutions. As the concentration of the dye in the solution approached zero, the activity coefficient approached unity Eq. (11)

$$\lim_{C_e \to 0} \frac{q_e}{C_e} = K_0 \tag{11}$$

The values of K_0 determined from the intercept (figure not shown), by plotting ln q_e/C_e versus Ce and extrapolating to $C_e = 0$ (Gupta et al., 2004). All the calculated thermodynamic parameters are presented in Table 2.

For the adsorption of both GRL and DY 12 dyes on CSAC, the obtained ΔH values were negative, which indicated the exothermic nature of both dye adsorption onto CSAC. The change in entropy was positive, indicating the entropy of the system increased during the adsorption. However, it should also be noted that the entropy of the universe (including the system and the surroundings) might increase because the adsorption reaction was not an isolated process. The negative values of $\Delta G°$ for both dyes demonstrated that the adsorption

Please cite this article in press as: Aljeboree, A.M. et al., Kinetics and equilibrium study for the adsorption of textile dyes on coconut shell activated carbon. Arabian Journal of Chemistry (2014), http://dx.doi.org/10.1016/j.arabjc.2014.01.020

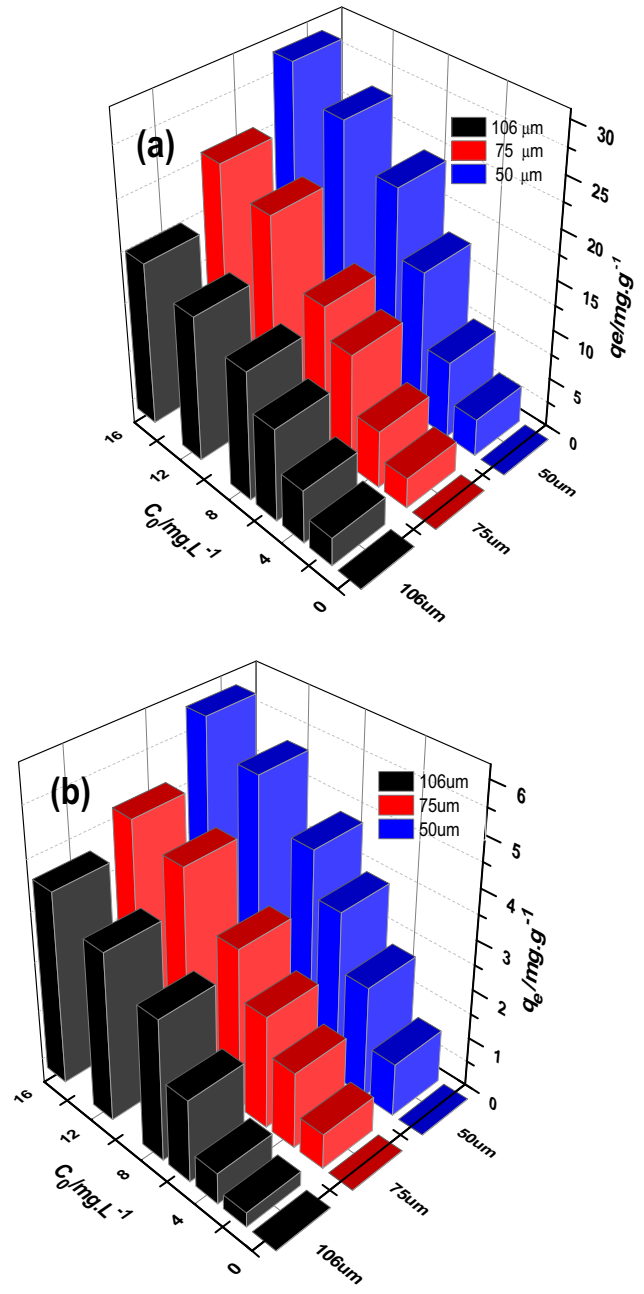

Figure 7 Effect of particle size on adsorption (a) GRL, and (b) DY 12 experimental conditions: Temp. 293 K, mass dosage 50 mg/L, and pH 6.

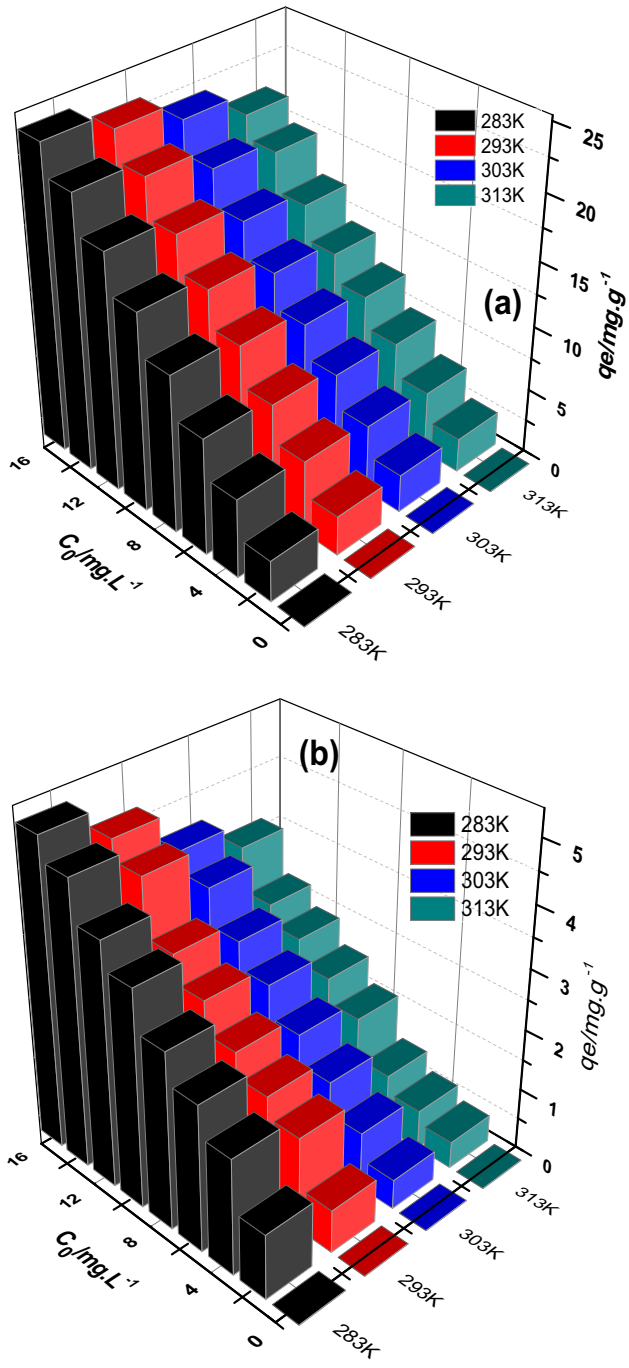

Figure 8 Effect of temperature on adsorption (a) GRL, and (b) DY 12: experimental conditions: particle size 75 µm, CSAC dosage 50 mg/L, and pH 6.

process on CSAC was a spontaneous process, and the decrease of $\Delta G°$ values with the increase of temperature indicated that the adsorption became less favorable at higher temperatures (Zhou et al., 2014).

3.5. Determination of adsorption isotherm parameters

The adsorption isotherm can describe the distribution of dye between solid phase and the solution at a certain temperature when the equilibrium was reached. The Langmuir, Freundlich, Temkin and Fritz–Schlunder (F–S) models were applied to fit the equilibrium data. Each isotherm model was expressed by relative certain constants which characterized the surface properties and indicated adsorption capacity of this material.

3.5.1. Langmuir isotherm

The Langmuir model proposes that monolayer sorption occurs on the solid surface with identical homogeneous sites

Table 2 Thermodynamic functions ΔG, ΔS and, ΔH of GRL and DY 12 adsorbed on the CSAC.

T/K	K_e	$\Delta G°$/kJ mol^{-1}	$\Delta H°$/kJ mol^{-1}	$\Delta S°$/J.K^{-1} mol^{-1}
CSAC adsorbent/GRL adsorbate				
283	7.01126	−4.58224	−3.966277	2.110093
293	6.46867	−4.54794		
303	6.25687	−4.6193		
313	5.92734	−4.63096		
CSAC adsorbent/DY 12 adsorbate				
283	9.15672	−5.21038	−2.14019	10.84927
293	8.85693	−5.31341		
303	8.6671	−5.44017		
313	8.37077	−5.52919		

(Langmuir, 1918). It also suggests that no further adsorption takes place once the active sites are covered with dye molecules. The saturated monolayer isotherm is presented by the following equation:

$$q_e = \frac{q_m K_L C_e}{1 + K_L C_e} \tag{12}$$

where C_e is the concentration of dye at equilibrium in solution (mg/L); q_e is unit equilibrium adsorption capacity; q_m is the maximum dye uptake, giving the information about adsorption capacity for a complete monolayer (mg/g); and KL is a constant denoted the energy of adsorption and affinity of the binding sites (L/mg).

3.5.2. Freundlich isotherm

Freundlich isotherm is an empirical model assuming that the distribution of the heat on the adsorbent surface is nonuniform, namely a heterogeneous adsorption (Freundlich and Heller, 1939). The equation is stated as follows:

$$q_e = K_f C_e^{1/n} \tag{13}$$

where n and K_F [mg/g (L/mg)^n] are both the Freundlich constants giving an indication of adsorption intensity and capacity, respectively. The degree of non-linearity between solution concentration and adsorption is n dependent as follows: if the value of n is equal to unity, the adsorption is linear; if the value is below to unity, this implies that adsorption process is chemical; if the value is above unity adsorption is a favorable physical process (Kumar et al., 2010).

3.5.3. Temkin isotherm

The Temkin model proposes into account the effects of the interaction of the adsorbate and the adsorbing species (Tempkin and Pyzhev, 1940). By ignoring the extremely low and large concentration values, the model assumes that the heat of adsorption (a function of temperature) of all of the molecules in the layer would decrease linearly rather than logarithmically with coverage due to adsorbate–adsorbent interactions (Aharoni and Ungarish, 1977), the equation is stated as follows:

$$q_e = \frac{RT}{b} \log(K_T C_e) \tag{14}$$

where b Tempkin constant related to the heat of adsorption (kJ/mol), and K_T empirical Tempkin constant related to the equilibrium binding constant related to the maximum binding energy (L/mg).

3.5.4. Fritz–Schlunder (F–S) isotherm

The F–S model is empirical three-parameter isotherm combining the Langmuir and Freundlich isotherms (Fritz and Schlunder, 1974). It is based on the following equation:

$$q_e = \frac{K_{FS} q_m C_e}{1 + q_m C_e^n} \tag{15}$$

where K_{FS} is the Fritz–Schlunder model constant (L/mg), q_m the amount of dye adsorbed (mg/g) when the saturation is attained, and n is the Freundlich constant (Batzias and Sidiras, 2007).

The coefficients of determination (R^2) and isotherm parameters from nonlinear regressive method were listed in Table 3. A comparison of nonlinear fitted curves from experimental data and four different isotherms at 283, 293, 303 and 313 K is shown in Fig. 9.

The Langmuir adsorption model was found to fit the experimental data for both dyes sufficiently in accordance with the liner correlation coefficients (R^2). The larger values of R^2 ($\geqslant$0.9867) indicted the applicability of the Langmuir isotherm for dye adsorption. q_m was an important Langmuir constant, representing the maximum capacity at equilibrium. The difference of K_L values between CSAC/GRL and CSAC/DY 12 refers to the different in binding strength and capacity of the dyes with the surface of the CSAC, in general values of KL decreased with the rise of temperature.

The Freundlich model did not provide any information about the saturation adsorption capacity as well as Langmuir model with lower R^2 (0.9552). The parameters of K_F and $1/n$ exhibited intense change at higher temperatures. The values of $1/n$ ($0.1 < 1/n < 1$) indicated favorable adsorption of both dyes at experimental conditions. The Temkin model provides calculation of equilibrium binding constant corresponding to the maximum binding energy, K_T, decreased as the experimental temperature increased from 283 to 313 K, which implies that the adsorption process is exothermic and favored at higher temperatures. Moreover, it was observed from Fig. 9 that the fitted curves from the F–S isotherm were most near to the experimental data at experimental conditions. Hence, the (F–S) model was best to describe adsorption behavior at equilibrium. By comparing the four models, it seems that the model of Fritz–Schlunder is the most adapted for the fitting of adsorption isotherms, then Langmuir model more adapted

Please cite this article in press as: Aljeboree, A.M. et al., Kinetics and equilibrium study for the adsorption of textile dyes on coconut shell activated carbon. Arabian Journal of Chemistry (2014), http://dx.doi.org/10.1016/j.arabjc.2014.01.020

Table 3 Parameters for different parameters isotherm models for the adsorption study of GRL, and DY 12 dyes onto CSAC at different temperatures.

Isotherm models	Parameters	GRL dye				DY 12 dye			
		Temperature/K				Temperature/K			
		283	293	303	313	283	293	303	313
Langmuir	q_m ($mg.g^{-1}$)	51.55973 ± 4.6333	62.0622 ± 7.3265	58.2523 ± 5.4931	58.51038 ± 7.2047	9.9275 ± 0.6114	13.7752 ± 1.2896	10.0211 ± 0.4543	12.6067 ± 2.6766
	K_L($L.mg^{-1}$)	0.21508 ± 0.0304	0.12128 ± 0.02008	0.10311 ± 0.0136	0.08209 ± 0.0138	0.1338 ± 0.0170	0.0496 ± 0.0068	0.0694 ± 0.0052	0.0356 ± 0.0103
	R^2	0.9933	0.99449	0.99665	0.99518	0.98923	0.99544	0.99792	0.9867
Freundlich	K_F	9.13054 ± 0.5222	6.92385 ± 0.39591	5.74431 ± 0.2924	4.70083 ± 0.3218	1.5380 ± 0.1936	0.8089 ± 0.0741	0.8414 ± 0.0747	0.5120 ± 0.0762
	1/n	0.71021 ± 0.0521	0.77417 ± 0.04539	0.77352 ± 0.0363	0.79674 ± 0.0449	0.56417 ± 0.05781	0.7469 ± 0.0403	0.6824 ± 0.0390	0.8052 ± 0.0638
	R^2	0.97679	0.98592	0.99115	0.98701	0.95521	0.98817	0.98633	0.97579
Tempkin	b/$J.mole^{-1}$	2.9939 ± 0.2822	2.44113 ± 0.3910	2.16876 ± 0.361	1.67253 ± 0.2210	2.2226 ± 0.0960	2.1375 ± 0.1621	1.8524 ± 0.1042	1.7605 ± 0.1172
	K_T	9.13003 ± 0.5028	8.50254 ± 0.7920	7.79026 ± 0.7390	7.80985 ± 0.6289	1.2665 ± 0.1138	0.8337 ± 0.1110	0.9088 ± 0.0946	0.6708 ± 0.0718
	R^2	0.97915	0.94227	0.94023	0.95631	0.98709	0.96109	0.97825	0.96979
Fritz–Schlunder	qm	33.6805 ± 1.6735	40.48221 ± 6.4421	46.56237 ± 10.8049	33.70863 ± 3.0998	7.69475 ± 0.4405	10.58464 ± 2.2019	8.02541 ± 0.5816	6.01633 ± 0.6502
	K_{FS}	0.35858 ± 0.0247	0.1864 ± 0.0321	0.12808 ± 0.0304	0.13194 ± 0.0108	0.12999 ± 0.0104	0.05699 ± 0.0074	0.07556 ± 0.0035	0.04245 ± 0.0050
	m	1.33488 ± 0.0615	1.21833 ± 0.1149	1.08918 ± 0.1064	1.28034 ± 0.0744	1.34307 ± 0.1093	1.12811 ± 0.1235	1.14701 ± 0.0586	1.48367 ± 0.1420
	R^2	0.99892	0.99624	0.99649	0.99856	0.99589	0.99554	0.99891	0.99565

Please cite this article in press as: Aljeboree, A.M. et al., Kinetics and equilibrium study for the adsorption of textile dyes on coconut shell activated carbon. Arabian Journal of Chemistry (2014), http://dx.doi.org/10.1016/j.arabjc.2014.01.020

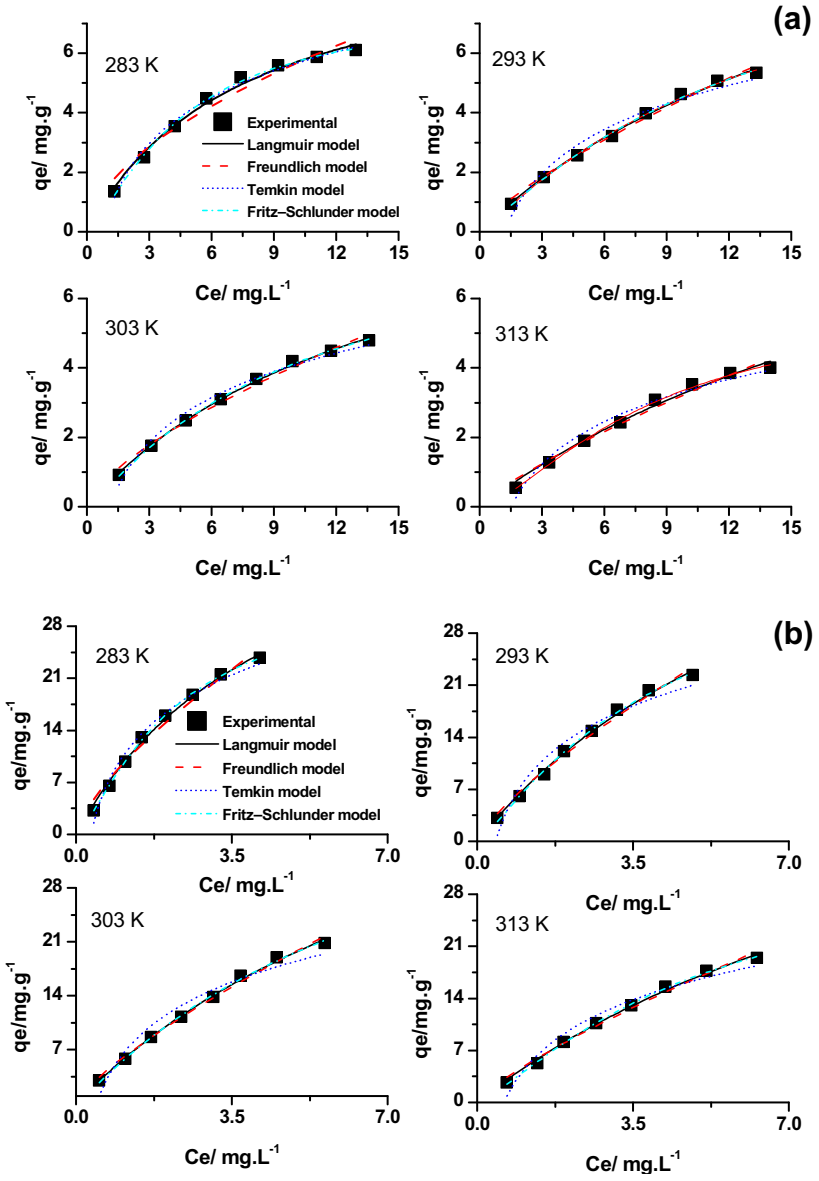

Figure 9 Adsorption isotherm models fitted to experimental adsorption of (a) DY 12, and (b) GRL (pH 6, Temp. 298, particle size 75 μm, mass dosage 50 mg/L).

than Temkin and Fruendlich models. The calculated parameters of fourth models are illustrated in Table 3.

4. Conclusion

Coconut shell, a food solid waste, was successfully utilized as a low cost alternative adsorbent for the removal of hazardous textile dyes (GRL and DY 12). The shifting of peaks in FTIR spectrum confirmed the GRL and DY 12 dye adsorption onto CSAC. The SEM study also made support to it by observing difference in surface morphology of adsorbent before and after adsorption of GRL and DY 12. Kinetics adsorption models of both GRL and DY 12 dyes on CSAC were studied and modeled using fourth kinetic models. The classification of the kinetic models according to the simulation of the adsorption study is: Chemisorption > Psuedo-second order > pseudo-first order > Intra-particle-diffuse. Also adsorption isotherms of these dyes on CSAC were studied and modeled using fourth isotherm models with more than two-parameter. An excellent prediction in all the studied concentration ranges can be obtained by the three-parameter equation (Fritz–Schlunder). The classification of the models according to the simulation of the adsorption isotherms is: Fritz–Schlunder > Langmuir > Freundlich > Tempkin. Thermodynamic study demonstrates the spontaneous and exothermic nature of adsorption process due to negative values of both free energy change and enthalpy change.

Acknowledgments

The authors acknowledges to Ministry of Higher Education and Scientific Research, Babylon University/College of Sciecne, Department of Chemistry, Iraq.

References

Acharya, J., Sahu, J.N., Sahoo, B.K., Mohanty, C.R., Meikap, B.C., 2009. Removal of chromium(VI) from wastewater by activated carbon developed from Tamarind wood activated with zinc chloride. Chem. Eng. J. 150, 25–39.

Aharoni, C., Ungarish, M., 1977. Kinetics of activated chemisorption. Part 2. Theoretical models. J. Chem. Soc., Faraday Trans. 73, 456–464.

Ahmad, M.A., Rahman, N.K., 2011. Equilibrium, kinetics and thermodynamic of Remazol Brilliant Orange 3R dye adsorption on coffee husk-based activated carbon. Chem. Eng. J. 170, 154–161.

Al-Degs, Y.S., El-Barghouthi, M.I., El-Sheikh, A.H., Walker, G.M., 2008. Effect of solution pH, ionic strength, and temperature on adsorption behavior of reactive dyes on activated carbon. Dyes Pigments 77, 16–23.

AlOthman, Z.A., Habila, M.A., Ali, R., Abdel, A., 2013. Ghafar, M.S. El-din Hassouna, Valorization of two waste streams into activated carbon and studying its adsorption kinetics equilibrium isotherms and thermodynamics for methylene blue removal. Arabian Journal of Chemistry 2, 2–12, http://dx.doi.org/10.1016/j.arabjc.2013.05.007.

Auta, M., Hameed, B.H., 2011. Optimized waste tea activated carbon for adsorption of methylene blue and acid blue 29 dyes using response surface methodology. Chem. Eng. J. 175, 233–243.

Banerjee, S., Chattopadhyaya, M.C., 2013. Adsorption characteristics for the removal of a toxic dye tartrazine from aqueous solutions by a low cost agricultural by-product. Arabian Journal of Chemistry, http://dx.doi.org/10.1016/j.arabjc.2013.06.005.

Batzias, F.A., Sidiras, D.K., 2007. Simulation of dye adsorption by beech sawdust as affected by pH. J. Hazard. Mater. 141, 668–679.

Cazetta, A.L., Vargas, A.M., Nogami, E.M., Kunita, M.H., Guilherme, M.R., Martins, A.C., Silva, T.L., Moraes, J.G., Almeida, V.C., 2011. NaOH-activated carbon of high surface area produced from coconut shell: Kinetics and equilibrium studies from the methylene blue adsorption. Chem. Eng. J. 174, 117–125.

Chiou, M., Chuang, G., 2006. Competitive adsorption of dye metanil yellow and RB15 in acid solutions on chemically cross-linked chitosan beads. Chemosphere. 62, 731–740.

Demirbas, E., Kobya, M., Sulak, M.T., 2008. Adsorption kinetics of a basic dye from aqueous solutions onto apricot stone activated carbon. Bioresour. Technol. 99, 5368–5373.

Dotto, G.L., Lima, E.C., Pinto, L.A., 2012. Biosorption of food dyes onto Spirulina platensis nanoparticles: Equilibrium isotherm and thermodynamic analysis. Bioresour. Technol. 103, 123–130.

Foo, K.Y., Hameed, B.H., 2012. Coconut husk derived activated carbon via microwave induced activation: Effects of activation agents, preparation parameters and adsorption performance. Chem. Eng. J. 184, 57–65.

Freundlich, H., Heller, W., 1939. The adsorption of cis- and trans-azobenzene. J. Am. Chem. Soc. 61, 2228–2230.

Fritz, W., Schlunder, E.U., 1974. Simultaneous adsorption equilibria of organic solutes in dilute aqueous solutions on activated carbon. Chem. Eng. Sci. 29, 1279–1282.

Geegel, U., Kolancilar, H., 2012. Adsorption of Remazol brilliant blue R on activated carbon prepared from a pine cone. Nat. Prod. Res. 26, 659–664.

Ghaedi, M., Sadeghian, B., Pebdani, A.A., Sahraei, R., Daneshfar, A., Duran, C., 2012. Kinetics, thermodynamics and equilibrium evaluation of direct yellow 12 removal by adsorption onto silver nanoparticles loaded activated carbon. Chem. Eng. J. 187, 133–141.

Ghaedi, M., Ansari, A., Sahraei, R., 2013. ZnS:Cu nanoparticles loaded on activated carbon as novel adsorbent for kinetic, thermodynamic and isotherm studies of reactive orange 12 and direct yellow 12 adsorption. Spectrochim Acta A Mol. Biomol. Spectrosc. 114, 687–694.

Gouamid, M., Ouahrani, M.R., Bensaci, M.B., 2013. Adsorption equilibrium, kinetics and thermodynamics of methylene blue from aqueous solutions using date palm leaves. Energy Procedia 36, 898–907.

Gupta, V.K., Singh, P., Rahman, N., 2004. Adsorption behavior of Hg(II), Pb(II), and Cd(II) from aqueous solution on Duolite C-433: a synthetic resin. J. Colloid Interf. Sci. 275, 398–402.

Hajati, S., Ghaedi, M., Karimi, F., Barazesh, B., Sahraei, R., Daneshfar, A., 2014. Competitive adsorption of direct yellow 12 and reactive o12 on ZnS:Mn nanoparticles loaded on activated carbon as novel adsorbent. J. Ind. Eng. Chem. 20, 564–571.

Hameed, K.S., Muthirulan, P., Meenakshi, S.M., 2013. Adsorption of chromotrope dye onto activated carbons obtained from the seeds of various plants: Equilibrium and kinetics studies. Arabian J. Chem, http://dx.doi.org/10.1016/j.arabjc.2013.07.058.

Ho, Y.S., McKay, G., 1999. Pseudo-second order model for sorption processes. Process Biochem. 34, 451–465.

Iqbal, M.J., Ashiq, M.N., 2007. Adsorption of dyes from aqueous solutions on activated charcoal. J. Hazard. Mater. 139, 57–66.

Iqbal, J., Wattoo, F.H., Wattoo, M.S., Malik, R., Tirmizi, S.A., Imran, M., Ghangro, A.B., 2011. Adsorption of acid yellow dye on flakes of chitosan prepared from fishery wastes. Arabian J. Chem. 4, 389–395.

Khaled, A., El Nemr, A., Ei-Sikaily, A., Abdelwahab, A., 2009. Treatment of artificial textile dye effluent containing direct yellow 12 by orange peel carbon. Desalination 238, 210–232.

Kilic, M., Apaydin-Varol, E., Putun, E.A., 2011. Adsorptive removal of phenol from aqueous solutions on activated carbon prepared from tobacco residues: Equilibrium, kinetics and thermodynamics. J. Hazard. Mater. 189, 397–403.

Kismir, Y., Aroguz, A.Z., 2011. Adsorption characteristics of the hazardous dye brilliant green on Saklikent mud. Chem. Eng. J. 172, 199–206.

Konicki, W., Sibera, D., Mijowska, E., Lendzion-Bielun, Z., Narkiewicz, U., 2013. Equilibrium and kinetic studies on acid dye acid red 88 adsorption by magnetic $ZnFe_2O_4$ spinel ferrite nanoparticles. J. Colloid Interf. Sci. 398, 152–160.

Kumar, P.S., Ramalingam, S., Senthamarai, C., Niranjanaa, M., Vijayalakshmi, P., Sivanesan, S., 2010. Adsorption of dye from aqueous solution by cashew nut shell: studies on equilibrium isotherm, kinetics and thermodynamics of interactions. Desalination 261, 52–60.

Lagergren, S., 1898. About the theory of so-called adsorption of soluble substances. Kungliga Suensk Vetenskapsakademiens Handlingar 241, 1–39.

Langmuir, I., 1918. Adsorption of gases on plain surfaces of glass mica platinum. J. Am. Chem. Soc. 40, 1361–1403.

Li, Q., Yue, Q., Su, Y., Gao, B., Sun, H., 2010. Equilibrium, thermodynamics and process design to minimize adsorbent amount for the adsorption of acid dyes onto cationic polymer-loaded bentonite. Chem. Eng. J. 158, 489–497.

Li, W., Yue, Q., Tu, P., Ma, Z., Gao, B., Li, J., Xu, X., 2011. Adsorption characteristics of dyes in columns of activated carbon prepared from paper mill sewage sludge. Chem. Eng. J. 178, 197–203.

Li, H., Huang, G., An, C., Hu, J., Yang, S., 2013. Removal of tannin from aqueous solution by adsorption onto treated coal fly ash: kinetic, equilibrium, and thermodynamic studies. Ind. Eeg. Chem. Res. 52, 15923–15931.

Low, M.D., 1960. Kinetics of chemisorption of gases on solids. Chem. Rev. 60, 267–312.

Malik, R., Ramteke, D.S., Wate, S.R., 2007. Adsorption of malachite green on groundnut shell waste based powdered activated carbon. Waste Manage. 27, 1129–1138.

Namasivayam, C., Kavitha, D., 2002. Removal of Congo red from water by adsorption onto activated carbon prepared from coir pith, an agricultural solid waste. Dyes Pigments 54, 47–58.

Prahas, D., Kartika, Y., Indraswati, N., Ismadji, S., 2008. Activated carbon from jackfruit peel waste by H_3PO_4 chemical activation: pore structure and surface chemistry characterization. Chem. Eng. J. 140, 32–42.

Rehman, M.S., Munir, M., Ashfaq, M., Rashid, N., Nazar, M.F., Danish, M., Han, J., 2013. Adsorption of brilliant green dye from aqueous solution onto red clay. Chem. Eng. J. 228, 54–62.

Please cite this article in press as: Aljeboree, A.M. et al., Kinetics and equilibrium study for the adsorption of textile dyes on coconut shell activated carbon. Arabian Journal of Chemistry (2014), http://dx.doi.org/10.1016/j.arabjc.2014.01.020

Royer, B., Cardoso, N.F., Lima, E.C., Vaghetti, J.P., Simon, N.M., Calvete, T., Veses, R.C., 2009. Applications of Brazilian pine-fruit shell in natural and carbonized forms as adsorbents to removal of methylene blue from aqueous solutions: kinetic and equilibrium study. J. Hazard. Mater. 164, 1213–1222.

Senthilkumaar, S., Kalaamani, P., Subburaam, C.V., 2006. Liquid phase adsorption of crystal violet onto activated carbons derived from male flowers of coconut tree. J. Hazard. Mater. 136, 800–808.

Shi, Y., Kong, X., Zhang, C., Chen, Y., Hua, Y., 2013. Adsorption of soy isoflavones by activated carbon: kinetics, thermodynamics and influence of soy oligosaccharides. Chem. Eng. J. 215–216, 113–121.

Tan, I.W., Ahmad, A.L., Hameed, B.H., 2008. Adsorption of basic dye using activated carbon prepared from oil palm shell: batch and fixed bed studies. Desalination 225, 13–28.

Tempkin, M.J., Pyzhev, V., 1940. Kinetics of ammonia synthesis on promoted iron catalysts. Acta Physicochim. URSS 12, 217–222.

Thinakaran, N., Baskaralingam, P., Pulikesi, M., Panneerselvam, P., Sivanesan, S., 2008. Removal of acid violet 17 from aqueous solutions by adsorption onto activated carbon prepared from sunflower seed hull. J. Hazard. Mater. 151, 316–322.

Tsai, W.T., Chang, C.Y., Lin, M.C., Chien, S.F., Sun, H.F., Hsieh, M.F., 2001. Adsorption of acid dye onto activated carbons prepared from agricultural waste bagasse by $ZnCl_2$ activation. Chemosphere 45, 51–58.

Visa, M., Bogatu, C., Duta, A., 2010. Simultaneous adsorption of dyes and heavy metals from multicomponent solutions using fly ash. Appl. Surf. Sci. 256, 5486–5491.

Weber, W.J., Morris, J.C., 1963. Kinetics of adsorption on carbon from solutions. J. Sanit. Eng. Div. 89, 31–60.

Yener, J., Kopac, T., Dogu, G., Dogu, T., 2006. Adsorption of basic yellow 28 from aqueous solutions with clinoptilolite and amberlite. J. Colloid Interf. Sci. 294, 255–264.

Zhou, L., Jin, J., Liu, Z., Liang, X., Shang, C., 2011. Adsorption of acid dyes from aqueous solutions by the ethylenediamine-modified magnetic chitosan nanoparticles. J. Hazard. Mater. 185, 1045–1052.

Zhou, Z., Lin, S., Yue, T., Lee, T., 2014. Adsorption of food dyes from aqueous solution by glutaraldehyde cross-linked magnetic chitosan nanoparticles. J. Food Eng. 126, 133–141.

Please cite this article in press as: Aljeboree, A.M. et al., Kinetics and equilibrium study for the adsorption of textile dyes on coconut shell activated carbon. Arabian Journal of Chemistry (2014), http://dx.doi.org/10.1016/j.arabjc.2014.01.020